

# FitDiff: Robust monocular 3D facial shape and reflectance estimation using Diffusion Models

Stathis Galanakis<sup>✉</sup>, Alexandros Lattas<sup>✉</sup>, Stylianos Moschoglou<sup>✉</sup>, and Stefanos Zafeiriou<sup>✉</sup>

Imperial College London

**Abstract.** The remarkable progress in 3D face reconstruction has resulted in high-detail and photorealistic facial representations. Recently, Diffusion Models have revolutionized the capabilities of generative methods by surpassing the performance of GANs. In this work, we present FitDiff, a diffusion-based 3D facial avatar generative model. Leveraging diffusion principles, our model accurately generates relightable facial avatars, utilizing an identity embedding extracted from an “in-the-wild” 2D facial image. The introduced multi-modal diffusion model is the first to concurrently output facial reflectance maps (diffuse and specular albedo and normals) and shapes, showcasing great generalization capabilities. It is solely trained on an annotated subset of a public facial dataset, paired with 3D reconstructions. We revisit the typical 3D facial fitting approach by guiding a reverse diffusion process using perceptual and face recognition losses. Being the first 3D LDM conditioned on face recognition embeddings, FitDiff reconstructs relightable human avatars, that can be used as-is in common rendering engines, starting only from an unconstrained facial image, and achieving state-of-the-art performance. Please see our project page at [fitdiff.github.io](https://fitdiff.github.io).

**Keywords:** 3D Face Reconstruction · Face Analysis · Diffusion Models

## 1 Introduction

A fundamental objective of Computer Vision encompasses photorealistic 3D face reconstruction from a single image, which has gained significant attention from the research community over the past few decades. Its numerous applications in computer graphics, virtual reality, and entertainment, include avatar creation, face animation and manipulation [1, 4, 27, 57, 87]. Despite the notable recent progress, accurate replication of personalized facial reconstructions continues to present a challenge. This is primarily due to the inherent ambiguity present in monocular images, as well as the difficulties associated with handling occlusions and capturing substantial variations in lighting conditions and facial expressions. On top of that, captured 3D facial datasets are still relatively small [106], including biases and lacking generalization in parallel with structural limitations of the current facial reconstruction methods.

The 3D Morphable Model (3DMM) was introduced in the seminal work of Blanz and Vetter [6] and uses Principal Component Analysis (PCA) to model

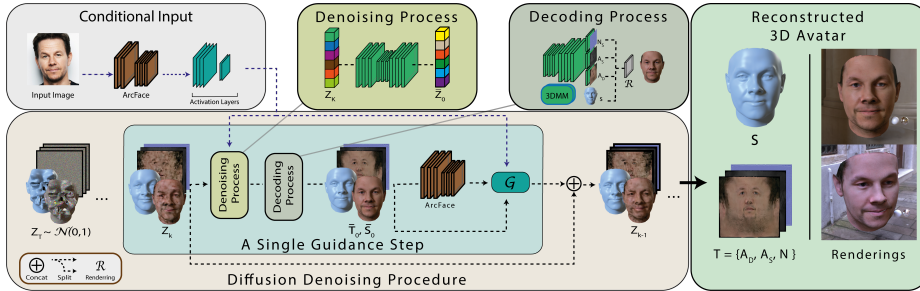


**Fig. 1:** Overview of FitDiff, a latent diffusion-based 3D facial generative network. Starting from Gaussian noise, our method generates facial avatars with relightable reflectance and shape, conditioned on an identity embedding. During sampling, a novel guidance algorithm is applied for further control of the resulting identity.  $Z_T, Z_k$  and  $Z_{k-1}$  are visualized in the actual picture space for illustration purposes.

the complex facial shapes and textures of 200 facial scans. Since then, there has been tremendous progress in retrieving 3D facial information from a monocular image like large-scale statistical models utilizing hundreds of subjects [8, 50, 68]. Even though most statistical models can accurately reconstruct the facial shape, they do not perform well in capturing the facial texture [8]. More recently, Generative Adversarial Networks (GANs) [31], and particularly the style-based generators [38–40], have demonstrated effectiveness in capturing intricate frequencies. This success has resulted in numerous subsequent studies combining these methods with 3DMMs [25, 27, 28], where the facial texture is modeled as a UV map. A fundamental challenge inherent in optimization fitting methods is their susceptibility to outliers, requiring to heuristically initialize the GAN’s  $\mathbf{z}$  or  $\mathbf{w}$  embedding for the back-propagation during inference to avoid instabilities [47]. Additionally, they suffer from problems like unstable training and mode collapse [42, 78].

A solution to the aforementioned problems is the integration of the recent emerging Diffusion Models (DMs) [33]. These architectures have gained a lot of attention lately, because of their current state-of-the-art performance in image synthesis tasks [19]. Taking inspiration from the thermodynamics [82], DMs define a  $T$ -length Markov Chain by gradually adding normally distributed random noise to the data and learn to predict the input noise for each step  $t \in \{1, 2, \dots, T\}$ . They synthesize new data by reversing the diffusion process, starting from a normally distributed random noise and progressively denoising it. This methodology has already been applied to synthesize and manipulate facial images [64, 95, 102]. Nevertheless, it is noteworthy to emphasize that most of these methods employ a conditional mechanism reliant on textual descriptions or other auxiliary information [71], thereby directing their attention not exclusively towards the faithful reconstruction of input facial identity and the exploration of the potential of robust identity embeddings. Moreover, Relightify [64] requires partially completed facial UV maps and third-party extracted facial shapes as input, thus being prone these third-party failures.

This study presents FitDiff, the first multi-modal generative model that synthesizes high-fidelity facial avatars given only an input facial image, starting from randomly initialized Gaussian noise. By harnessing the impressive generation capabilities of LDMs [76], we delve into their potential in the field of 3D facial reconstruction. Our approach enables the synthesis of facial avatars by combining facial UV reflectance maps and facial geometry while utilizing an identity embedding layer as a conditioning mechanism. The diffusion process is applied to the concatenation of the latent vectors of the facial texture maps and shape, while a VQGAN AutoEncoder [21] and a 3DMM model (LSFM [8]) are used to decode them. Moreover, we present a novel facial guidance algorithm incorporated into the reverse diffusion process for accurately reconstructing a target facial identity. FitDiff generates high-fidelity facial avatars while achieving a state-of-the-art identity preservation score. The training of our model involves fitting a facial reconstruction network [44] to a manually selected and curated set of images acquired from the CelebA-HQ dataset [37]. The fitting process results in acquiring facial shape and facial reflectance maps. Overall, in this paper:

- We introduce FitDiff, a multi-modal diffusion-based generative model that jointly produces facial geometry and appearance. The facial appearance consists of facial diffuse albedo, specular albedo, and normal maps, enabling photorealistic rendering.
- We show the first diffusion model conditioned on identity embeddings, acquired from an off-the-shelf face recognition network, whilst introducing a SPADE [66]-conditioned UNet architecture.
- We present unconditional samples of relightable avatars, but most importantly, we achieve facial reconstruction from a single “in-the-wild” image through identity embedding conditioning and guidance.

## 2 Related Work

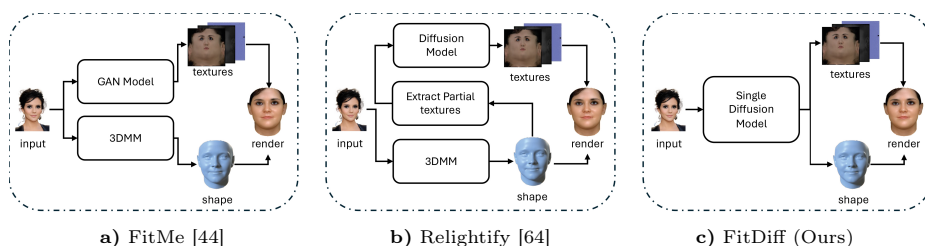


**Fig. 2:** Differences with existing state-of-the-art methods [44, 64]: Prior works rely on multiple separate models, which can fail on challenging inputs (Fig. 10). In contrast, our method uses only a single Latent Diffusion Model for both shape and reflectance textures prediction, achieving simplified architecture, training, and robustness.

## 2.1 Face Modeling

A wide variety of works followed the introduction of the emblematic first 3D Morphable Model (3DMM) [6] trained on 200 distinct subjects. Numerous works have since proposed improvements, especially on realistic expressions [3, 10, 11, 13, 48–50, 90, 99], large-scale dataset and model releases [9, 17, 68, 81]. However, those models were unable to capture high-frequency details due to their linear nature. To deal with this, many studies integrated 3DMMs with Deep Neural Networks [88, 92], Mesh Convolutions [60], GANs [26–28] and VAEs [5, 54, 74, 96]. Additionally, the photorealistic rendering of implicit representation-based methods [58, 65] led to numerous approaches [4, 23, 24, 35, 57, 62, 100]. However, their applications and editability remain challenging, hence this work focuses on explicit representations. Emphasizing the acquisition of highly detailed facial texture and faithful reflectance maps, Avatarme [43] and AvatarMe++ [45] treat the facial texture as a combination of diffuse albedo, specular albedo and normals UV maps whereas ReflectanceMM [32] models spatially varying BRDF, while trained in low-cost acquired data. In a different vein, the authors of MICA [106] leverage a robust face recognition network [18] with the objective of generating facial shapes. In [97], dense facial landmarks were introduced for better shape reconstruction, whilst a transformer-based facial reconstruction network was introduced in [104]. The aforementioned techniques and more recent methodologies [15, 22, 46, 72], which utilize displacement maps for finer facial shape details, consistently achieve state-of-the-art performance in facial shape competitions such as NoW [79] and REALY [14]. However, many of these approaches either produce facial texture with baked illumination or fail to generate it altogether. Recent works such as [20, 44, 55] aim to concurrently reconstruct facial shape and texture but still rely on separate dedicated models for each component (Fig. 2). Closer to our work is AlbedoGAN [72], which introduces a single network for acquiring both facial shape and texture. However, the proposed methodology generates maps containing baked illumination and cannot handle wearables, contrary to our approach.

## 2.2 Diffusion Models

Inspired by [82, 84–86], the authors of [19] showed that DMs can perform better than the widely used GAN-based methods in image synthesis tasks. DMs learn to model a data distribution  $\mathcal{P}(x)$  by gradually injecting normally distributed noise as a  $T$ -length Markov Chain and predicting the denoised data in each step. The reverse denoising process can be used as the sampling procedure. The high-quality samples and the more stable training have attracted the attention of the research community leading to a great variety of applications in image generation [34, 73, 76], text-to-image [41, 61], text-to-3D [70], Pointcloud [56, 101, 105] and Mesh [53] generation. One significant limitation of DMs is their sampling speed, which is hindered by their iterative generative nature. Despite the introduction of DDIMs [83], which helped decrease sampling time, a significant amount of computational resources is still necessary for each iteration step. Initial

approaches like [80, 93] and then Latent Diffusion Models (LDMs) [76] perform the diffusion process in the latent space, instead of the pixel space, while achieving comparable performance in image synthesis. Extensions of those methods broaden the applications into medicine [69], text-to-audio [52], and video creation [7]. On top of that, some approaches [51, 98] use a pre-trained LDM as priors. Closest to our work, other diffusion-based facial models [64, 95, 102] were presented. The former two employ a coarse-to-fine approach to attain identity information, unlike our single-stage methodology. Furthermore, Rodin [95] uses an implicit representation [16] for facial shape but doesn’t prioritize faithful reconstruction of the input facial identity. On the contrary, FitDiff integrates a fully-controllable 3DMM model, facilitating the generation of high-quality facial avatars that accurately represent the input identity. On the other hand, Relightify [64] uses an unconditional denoising network for filling partially completed facial UV maps extracted from third-party models. Although it may seem similar to our proposed methodology, FitDiff has several advantages over Relightify, which we discuss in detail in Section 6.

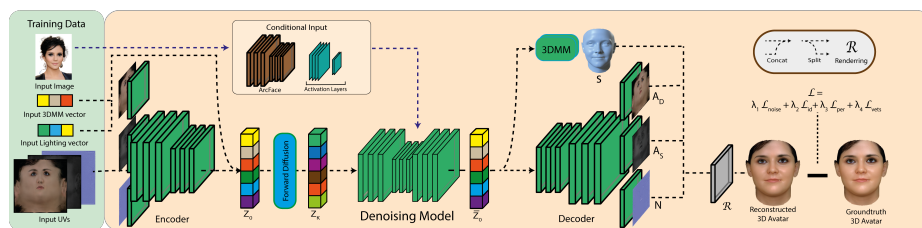


**Fig. 3:** Overview of the main phase of our training scheme: During each training iteration, the facial reflectance maps are initially projected onto the latent space and subsequently concatenated to the latent vector  $z_0$ , to which noise is introduced. Following the estimation of the initial  $\bar{z}_0$ , perceptual and face recognition losses are imposed upon the estimated initial avatar.

### 3 Method

In this work, we propose FitDiff, a latent-diffusion-based approach to reconstruct facial avatars. We harness the power of diffusion models for the generative and fitting process as, by nature, they are very robust in both processes since they directly operate on the image space [76]. On the other hand, GANs suffer from various issues such as mode collapse during training [89] or unrealistic outputs in fitting methods, resulting in unnecessary heuristics [44] to stabilize the outputs at the expense of fidelity.

A facial avatar can be formulated as a combination of a mesh  $\mathbf{S}$ , and texture  $\mathbf{T}$  which is defined as a combination of facial reflectance UV maps, namely diffuse albedo ( $\mathbf{A}_D$ ), specular albedo ( $\mathbf{A}_S$ ) and normals ( $\mathbf{N}$ ). Also, let us denote an “in-the-wild” image containing a face as  $\mathbf{I}$ , and  $\mathbf{V}_{trgt}$  as the corresponding target identity embedding of the appearing face. Given  $\mathbf{V}_{trgt}$  as input, FitDiff

generates a 3D facial avatar of the same identity as the one in  $\mathbf{I}$ , alongside with the current scene’s illumination parameters (ambient, diffuse, and specular lighting and lighting direction). An overview of our method is illustrated in Fig. 1, whereas the rest of the section includes a detailed presentation of our method’s architecture (Sec. 3.1), the proposed conditional input (Sec. 3.2), the training scheme (Sec. 3.3), and finally the identity-guidance sampling procedure (Sec. 3.4).

### 3.1 Model Architecture

FitDiff is a latent-diffusion based approach [76]. This is motivated by the challenges posed by the large number of parameters and the computational expenses associated with generating multiple meshes and texture images simultaneously. Thus, we represent facial avatars as a latent vector containing latent information about the shape, facial texture, and scene illumination:  $\mathbf{z} = \{\mathbf{z}_{tex} | \mathbf{z}_{shp} | \mathbf{z}_{ill}\} \in \mathbb{R}^{4288}$ , where  $\mathbf{z}_{tex} \in \mathbb{R}^{4096}$  signifies the facial reflectance latent vector,  $\mathbf{z}_{shp} \in \mathbb{R}^{183}$  the latent shape vector and  $\mathbf{z}_{ill} \in \mathbb{R}^9$  the scene illumination parameters. The latent shape vector  $\mathbf{z}_{shp}$  can be further separated into the identity parameters  $\mathbf{z}_{shp_i} \in \mathbb{R}^{158}$  and expression parameters  $\mathbf{z}_{shp_e} \in \mathbb{R}^{25}$ .

FitDiff is composed of a 3D statistical model  $\mathcal{F}_{shp}$  (LSFM [8]) that generates facial geometry, a branched multi-modal AutoEncoder [21, 76] that generates facial reflectance maps and a denoising UNet AutoEncoder [77]. For a set of identity  $\mathbf{z}_{shp_i}$  and expression  $\mathbf{z}_{shp_e}$  parameters, the PCA face model  $\mathcal{F}_{shp}$  generates a facial mesh  $\mathbf{S}$  following the formula:

$$\mathbf{S} = \mathcal{F}_{shp}(\mathbf{z}_{shp}) = \mathbf{U}_i \cdot \mathbf{z}_{shp_i} + \mathbf{U}_e \cdot \mathbf{z}_{shp_e} + \mathbf{m}_i$$

where  $\mathbf{U}_i$  and  $\mathbf{U}_e$  are the identity and expression bases, respectively, and  $\mathbf{m}_s$  is the mean face. Additionally, we incorporate a robust branched VQGAN [21, 76], to function as a multi-modal texture UV generator. More specifically, the VQGAN encoder  $\mathcal{E}$  concurrently encodes facial diffuse albedo  $\mathbf{A}_D$ , specular albedo  $\mathbf{A}_S$  and normals  $\mathbf{N}$  into the same latent vector  $\mathbf{z}_{tex}$ , whereas the VQGAN decoder  $\mathcal{D}$  reconstructs them given the input latent vector  $\mathbf{z}_{tex}$ . Finally, following common diffusion-based methods [19, 33, 76], we utilize a UNet AutoEncoder [77] with self-attention [94] layers  $e_\theta(x_t, t)$  conditioned to the input time step  $t \in \{1, \dots, T\}$ . We train the UNet to predict the injected noise  $\epsilon$ , sampled from a standard normal distribution, i.e.,  $\epsilon \sim \mathcal{N}(\mathbf{0}, \mathbf{1})$ . The training details of our method are presented in Sec. 3.3.

### 3.2 Conditional input

In the underlying UNet model, we integrate a powerful conditioning mechanism to effectively learn all the necessary identity information. An ideal identity embedding must contain both low and high-frequency information aiming to accurately reconstruct the desired facial avatar. To acquire such an identity embedding, we employ a powerful identity recognition network [18], to which we

feed the input facial image. Then, the resulting conditioning vector is a combination of the last feature vector with the intermediate activation layers of the identity recognition network.

Let  $\mathcal{C}^n$  be the  $n$ -th intermediate layer of the identity recognition network. We extract the intermediate activation maps  $\mathcal{C}^2 \in \mathbb{R}^{128 \times 28 \times 28}$ ,  $\mathcal{C}^3 \in \mathbb{R}^{256 \times 14 \times 14}$ ,  $\mathcal{C}^4 \in \mathbb{R}^{512 \times 7 \times 7}$  and concatenate them channel-wise with the identity embedding  $\mathbf{V} \in \mathbb{R}^{512}$ , which is expanded spatially. Because of the 2D nature of our identity embedding and following [23], we use SPADE layers [66] as a conditioning mechanism to inject the conditioning vector into the intermediate layers of the UNet.

### 3.3 Model Training

Our training scheme consists of two phases: Initially, we conduct the training for the branched texture AE, followed by the subsequent training for the denoising UNet model. The first part of our training protocol entails the training of the branched multi-modal AE [21], whereby triplets are employed as input data:

$$x = \{\mathbf{A}_D, \mathbf{A}_S, \mathbf{N}\}, \quad \mathbf{A}_D, \mathbf{A}_S, \mathbf{N} \in \mathbb{R}^{512 \times 512 \times 3}$$

where  $\mathbf{A}_D$  represents the diffuse albedo,  $\mathbf{A}_S$  the specular albedo and  $\mathbf{N}$  the normals. Our approach includes a branched multi-modal discriminator [44] in combination with a perceptual loss [103] as the training loss. The discriminator is a path-based discriminator [21] comprising two branches, to accommodate their different statistics [44]. The first branch gets as input the concatenation of diffuse and specular albedos  $\mathbf{A}_D \oplus \mathbf{A}_S$ , whereas the second branch receives the normals  $\mathbf{N}$ . Furthermore, we adhere to the default training parameters outlined in [76]. For a given triplet  $x_k$ , the encoder  $\mathcal{E}$  projects  $x_k$  into a latent representation  $\mathbf{z}_{tex} = \mathcal{E}(x_k)$ , where  $\mathbf{z}_{tex} \in \mathbb{R}^{h \times w \times c}$ . Then, the latent vector  $\mathbf{z}_{tex}$  is fed into the decoder  $\mathcal{D}$ , which produces a reconstructed output triplet  $\bar{x}_k$ . We downsample the input texture UVs by a factor of  $f = H/h = 512/64 = 8$ , following the downsampling investigations in [76] and due to computational limitations. For the shape decoder, we use an LSFm [8] model, pre-trained in  $\sim 10k$  identities.

After training the texture AutoEncoder, we freeze its weight parameters and embark on the training of the identity-conditioned UNet. A comprehensive overview of this training approach is presented in Fig. 3. During this phase, we employ multiple components including the identity embedding  $\mathbf{V}_{tgt}$ , the shape  $\mathbf{z}_{shp}$ , the distinct facial texture maps  $\mathbf{A}_D$ ,  $\mathbf{A}_S$ , and  $\mathbf{N}$ , and the scene lighting  $\mathbf{z}_{ill}$ . At each training step, the facial reflectance maps undergo an initial encoding by the pre-trained encoder  $\mathcal{E}$ , thereby yielding the latent texture vector  $\mathbf{z}_{tex}$ . Then, the input vectors are concatenated, i.e.,  $\mathbf{z}_0 = \{\mathbf{z}_{tex} | \mathbf{z}_{shp} | \mathbf{z}_{ill}\}$ . Let us denote  $\mathbf{z}_t$  the noisy counterparts of  $\mathbf{z}_0$ , resulting from  $t$  steps of noise injection. The UNet network gets  $\mathbf{z}_t$  as input, and learns to predict the injected noise following:

$$L_{noise} := \mathbb{E}_{\mathcal{E}(x), \epsilon \sim \mathcal{N}(0,1), t} [\|\epsilon - \epsilon_\theta(\mathbf{z}_t, t, \mathbf{V})\|] \quad (1)$$

where  $\epsilon$  is the ground-truth injected noise,  $\epsilon_\theta$  the predicted injected noise from  $\mathbf{z}_t$ ,  $t$  the diffusion time step, and  $\mathbf{V}$  signifies the 2D identity embedding vector as described in Sec. 3.2.

In addition to the primary loss function  $\mathcal{L}_{noise}$ , our training scheme integrates additional losses intended to enhance robustness, which are the identity losses [27, 44]  $\mathcal{L}_{id}$ ,  $\mathcal{L}_{per}$  and the shape loss  $\mathcal{L}_{verts}$ . Detailed definitions for those are provided in the supplemental. It is important to note that these auxiliary losses are not applicable to the latent variables. Thus, the estimated initial latent vector  $\bar{\mathbf{z}}_0$  is computed as:  $\bar{\mathbf{z}}_0 = \frac{\mathbf{z}_t - \sqrt{1 - \bar{\alpha}_t} \epsilon}{\sqrt{\bar{\alpha}_t}}$ . The vector  $\bar{\mathbf{z}}_0$  is further decoded into the estimated initial avatar. Firstly,  $\bar{\mathbf{z}}_0$  is split into the estimated initial latent texture vector  $\bar{\mathbf{z}}_{0_{tex}}$ , latent shape vector  $\bar{\mathbf{z}}_{0_{shp}}$  and scene parameters  $\bar{\mathbf{z}}_{0_{ill}}$ . The first two vectors are fed into the decoder  $\mathcal{D}$  and the PCA model  $\mathcal{F}_{shp}$  respectively. In this way, the estimated initial facial reflectance maps  $\bar{\mathcal{T}}_0$  and shape  $\bar{\mathcal{S}}_0$  are retrieved. Additionally, under the estimated initial scene illumination  $\bar{\mathbf{z}}_{0_{ill}}$ , we acquire the initial identity rendering  $\bar{I}_0$  using a differentiable renderer [75], while using a differentiable multi-texture map shader as introduced in [44, 45] under a single directional light. Overall, the conditional denoising model is trained using the following formula:

$$\mathcal{L} = \mathcal{L}_{noise} + \mathcal{L}_{id} + \mathcal{L}_{per} + \mathcal{L}_{verts}$$

where  $\mathcal{L}_{noise}$  is defined in Eq. 1,  $\mathcal{L}_{id}$  is the identity distance,  $\mathcal{L}_{per}$  the identity perceptual loss and  $\mathcal{L}_{verts}$  the shape loss.

Even though both the forward and the reverse diffusion processes can be described via stochastic differential equations in a continuous time [86], they can also be applied in discrete time by choosing a very small step, each time. The selection of the appropriate number of diffusion steps is based on the premise that, in the final step, the input data should be completely converted into random noise. We follow the training parameters proposed by the authors of [76] and we choose  $T = 1000$  while using a linear noise schedule. Furthermore, FitDiff is trained following the Classifier-Free approach [34]. This means that, during training, we randomly set the input identity embedding equal to zero with a probability of  $\mathcal{P}_{uncond} = 0.1$ .

### 3.4 Sampling Procedure

DMs generate new samples by reversing the diffusion process, commencing from an initial random Gaussian noise. In parallel, the authors of [83] introduced Denoising Diffusion Implicit Models (DDIMs) which are implicit probabilistic models [59]. They conduct a modified reverse diffusion process with fewer diffusion steps compared to those required during the vanilla DDPM sampling.

In our method, we adopt the DDIM sampling technique and integrate it into our trained architecture for the generation of facial avatars. We select the number of sampling steps to be  $T = 50$  for the DDIM sampling process. Aiming to generate accurate photorealistic avatars, we employ a novel guidance algorithm alongside the conditional input. Our approach is inspired by [19], in which the authors introduce a score corrector network conditioned on the diffusion step. In our implementation, we incorporate a face recognition network  $\mathcal{C}$  [18] as a score corrector alongside with an off-the-shelf facial landmark detector  $\mathcal{M}$  [12]



and a perceptual loss [103]. The guidance method can be implemented for the vanilla DDPM [19] and the DDIM [83] sampling techniques. For the generation of intermediate images, we employ a differentiable renderer [75] with the modifications introduced in [44, 45], under a single directional light. The pseudo-code and a detailed presentation of the proposed guidance method are presented in supplemental while the guidance formula is the following:

$$\mathcal{G} = \mathcal{G}_{id}^{cos} + \lambda_1 \mathcal{G}_{id}^{per} + \lambda_2 \mathcal{G}_{mse} + \lambda_3 \mathcal{G}_{lan} + \lambda_4 \mathcal{G}_{vgg} \quad (2)$$

where  $\mathcal{G}_{id}^{cos}$  denotes the cosine similarity between the identity vectors,  $\mathcal{G}_{id}^{per}$  the identity perceptual similarity,  $\mathcal{G}_{mse}$  the photometric loss,  $\mathcal{G}_{lan}$  is the distance between the 3D facial landmarks extracted by using  $\mathcal{M}$  [12] and  $\mathcal{G}_{vgg}$  is the perceptual similarity using [103]. Fig. 4 showcases examples of our method being applied to “in-the-wild” images.

## 4 Experiments

### 4.1 Dataset

Training such a diffusion model in a supervised manner requires a large dataset of labeled sets of facial images  $\mathbf{I}$ , facial textures  $\mathbf{T}$ , shape parameters  $\mathbf{z}_{shp}$  and facial recognition embeddings  $\mathbf{V}$ . Although a captured dataset could be used, there are no large enough public datasets [106]. As a workaround, we curate 9000 2D facial images from the CelebA-HQ Dataset [37]  $\mathbf{I}_i, i = 0 \dots 9 \cdot 10^3$ , on which we performed the following steps to acquire the labeled dataset: A) We use a state-of-the-art face recognition model [18], to extract the identity latent embeddings  $\mathbf{V}$ , which captures the facial structure, with minimal interference from shading, age, and accessories. B) We train a state-of-the-art StyleGAN-based [40] facial reconstruction network [44]  $\phi$ , on public datasets of facial textures [43, 63], and use the LSFM 3DMM for the facial shape [8]. Following an iterative optimization [44], we fit our model to the CelebA-HQ dataset [37] and acquire pseudo-ground truth facial textures, 3DMM shape weights, and scene illumination parameters

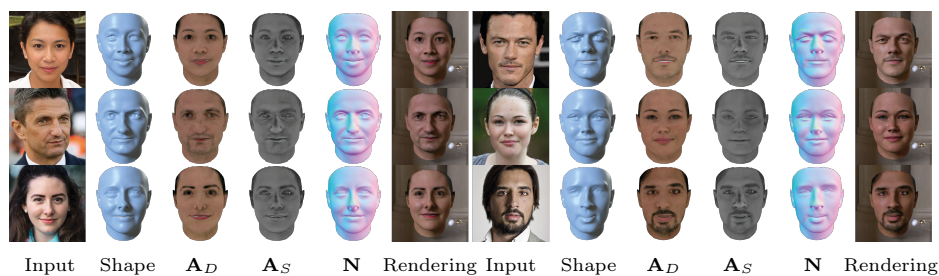


**Fig. 4:** Qualitative results of FitDiff on “in-the-wild” facial images, showing shape, reflectance, and environment map renderings.

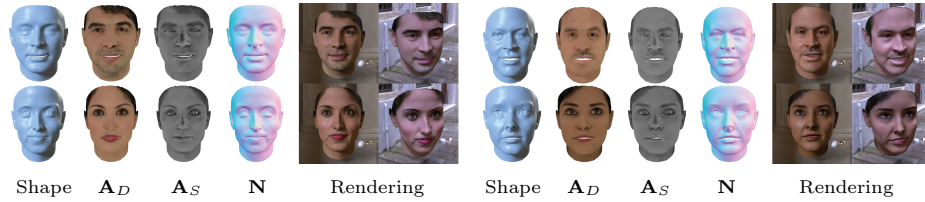


**Fig. 5:** Samples generated by FitDiff with unconditional sampling. Our method can generate diverse facial shapes and reflectance maps.

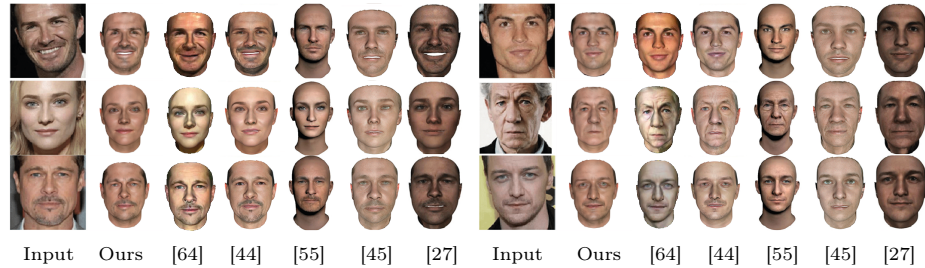


**Fig. 6:** Qualitative comparison between our method and other monocular-image facial reconstruction approaches [27, 44, 45, 55, 64]

$\phi(\mathbf{I}_i) \rightarrow \mathbf{A}_{D_i}, \mathbf{A}_{S_i}, \mathbf{N}_i, \mathbf{z}_{shp_i}, \mathbf{z}_{ill_i}$ . In the end, we acquire a dataset of paired images, facial reflectance textures, facial shape, scene illumination and latent vectors:  $\{\mathbf{I}_i, \mathbf{A}_{D_i}, \mathbf{A}_{S_i}, \mathbf{N}_i, \mathbf{z}_{shp_i}, \mathbf{z}_{ill_i}, \mathbf{V}_i\}$ .

## 4.2 Unconditional Sampling

As mentioned in Sec. 3.3, FitDiff is trained following the classifier-free guidance (CFG) [34] training scheme. In this manner, our method can generate completely random facial identities without any prior input or supervision. We present the unconditional generated diffuse albedos  $\mathbf{A}_D$ , specular albedos  $\mathbf{A}_S$ , normals  $\mathbf{N}$ , facial shapes  $\mathbf{S}$  and renderings in Fig. 5. This figure illustrates our method’s ability to create distinct shapes and textures. These assets hold significant potential for various applications, including enhancing existing datasets through augmentation and enrichment, as well as generating truly random identities for computer-based applications.

## 4.3 Qualitative comparisons

We compare our method’s generated samples with other monocular-image face reconstruction methods [27, 44, 45, 55, 64] and present the generated samples in Fig. 6. The majority of these techniques rely on GAN-based methods and employ fitting optimization procedures that encompass lighting, camera pose, and expression parameters, whereas Relightify [64] is the only diffusion-based approach. Our method can capture finer details than most of GAN-based methods ([27, 44, 45, 55]) whereas it generates equally detailed avatars like Relightify.

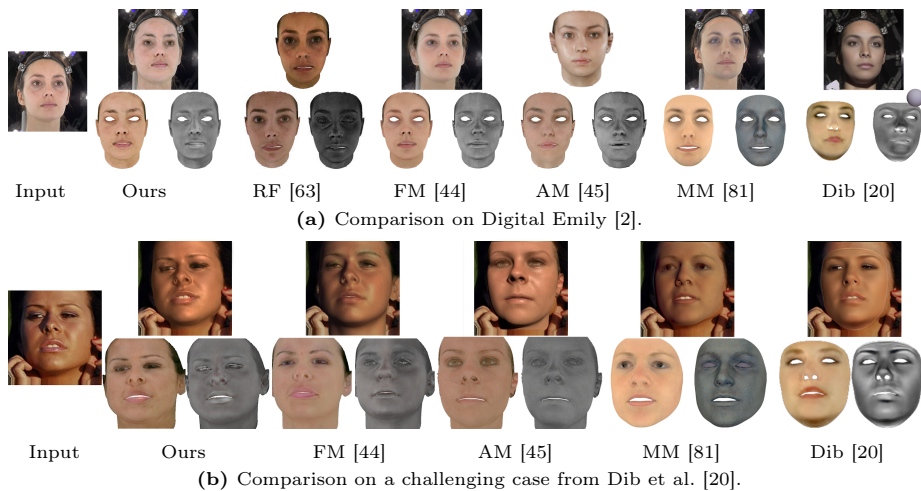


**Fig. 7:** Qualitative comparison on single-image reflectance acquisition against Relightify (RF) [64], FitMe (FM) [45], AvatarMe++ (AM) [45], AlbedoMM (MM) [81] and Dib et al. [20]. Up: overlaid rendering, Left: diffuse, Right: specular.

#### 4.4 Quantitative comparisons

**Facial Reflectance Acquisition Comparison** We evaluate the quality of our method’s generated facial reflectance maps by reconstructing 6 test subjects captured with a Light Stage [30]. We compare the generated diffuse albedos  $\mathbf{A}_D$ , specular albedos  $\mathbf{A}_S$  and normals  $\mathbf{N}$  with the respective ground truth, and MSE, PSNR, and SSIM distances are measured. We compare our method’s performance with AlbedoMM [81], AvatarMe++ [45] FitMe [44] and Relightify [64] and the results are presented in Tab. 1 and Fig. 7. FitDiff generates state-of-the-art shape normals, whereas it performs on par with Relightify [64] in the diffuse and specular albedo scenarios.

|         | Diffuse Albedo |              |              | Specular Albedo |              |              | Normals      |              |              |
|---------|----------------|--------------|--------------|-----------------|--------------|--------------|--------------|--------------|--------------|
|         | ↓MSE           | ↑PSNR        | ↑SSIM        | ↓MSE            | ↑PSNR        | ↑SSIM        | ↓MSE         | ↑PSNR        | ↑SSIM        |
| MM [81] | 0.028          | 15.82        | 0.595        | 0.007           | 21.24        | 0.608        | -            | -            | -            |
| AM [45] | 0.014          | 18.30        | 0.635        | 0.005           | 19.77        | 0.640        | 0.002        | 27.26        | 0.723        |
| FM [44] | 0.009          | 21.12        | 0.645        | 0.004           | 23.95        | 0.642        | 0.002        | 26.77        | 0.719        |
| RF [64] | 0.009          | <b>22.47</b> | 0.647        | <b>0.003</b>    | <b>27.17</b> | <b>0.710</b> | 0.002        | 26.69        | 0.719        |
| Ours    | <b>0.009</b>   | 21.16        | <b>0.647</b> | 0.004           | 24.30        | 0.645        | <b>0.001</b> | <b>28.74</b> | <b>0.734</b> |

**Table 1:** Quantitative comparison on 6 Light-Stage-captured data [30], between our method, AlbedoMM [81] (MM), AvatarMe++ [45] (AM), FitMe [44] (FM) and Relightify [64] (RF), measuring MSE, PSNR, and SSIM. Our method surpasses prior work in most cases or works on par with the current state-of-the-art in the rest.

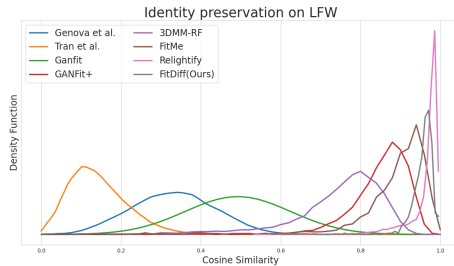


**Fig. 8:** We compare our approach with [23,27–29,44,64,91]. FitDiff performs on par with the current state-of-the-art method (Relightify [64]), while beating the rest.

| Method          | ID Sim.     |
|-----------------|-------------|
| Label Only      | 0.43        |
| CFG ( $w=2$ )   | 0.49        |
| CFG ( $w=9$ )   | 0.45        |
| <b>Guidance</b> | <b>0.88</b> |

**Table 2:** Ablation study on the identity similarity [18] performance of our method, with and without identity guidance.

**Identity preservation experiment** One of the key elements of our model is the ability to generate the facial identity depicted in the provided “in-the-wild” image. We quantitatively measure this by conducting an identity preservation experiment [23, 27–29]. We reconstruct the facial identities depicted in each image within the Labeled Faces in the Wild (LFW) dataset [36]. The reconstructed identities are fed into a face recognition network [67] and the identity cosine distance is measured by comparing their activation layers. As depicted in Fig. 8, FitDiff outperforms the previous state-of-the-art face-reconstruction methods [27, 44] and performs slightly less than current state-of-the-art method [64].

## 5 Ablation Study

### 5.1 Sampling guidance

Firstly, we examine the importance of the proposed facial guidance during the reverse diffusion process. To do so, we randomly pick about 100 “in-the-wild” images, and we consider three scenarios: a) sampling without any guidance, b) sampling using the classifier-free guidance [34] while using guidance scales  $w = \{2, 9\}$ , and c) our proposed method. The identity similarity scores are presented in Tab. 2, whereas visualizations of the generated examples are included in Fig. 9. The guidance algorithm demonstrates superior reconstruction performance compared to alternative methodologies.

### 5.2 Use of the conditioning mechanism

Another ablation study includes the necessity of our conditioning mechanism. We compare the texture information between the generated samples with and without our conditioning mechanism and examples of those are presented in Fig. 9d and 9e, respectively. These examples clearly show that finer details can be generated only when the corresponding identity embedding is used as input.

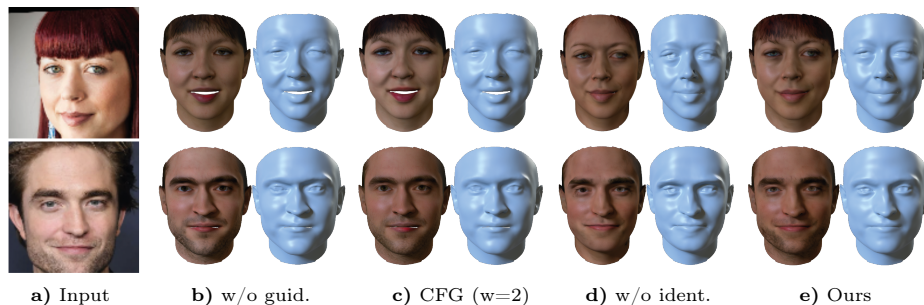


**Fig. 9:** Ablation study: Given the input images (a), we present corresponding samples without the guidance algorithm (b), samples using CFG with  $w=2$  (c) without the identity embedding (d) and finally our method (e).

## 6 Discussion

FitDiff is a latent diffusion model, which concurrently carries out facial shape and texture generation as a combination of diffuse albedo, specular albedo, and shape normals. A close work to ours is Relightify [64], which only generates facial texture UV maps, modeled like ours. Given partially completed facial texture maps and acquired facial shape, this method can very efficiently reconstruct completed facial UV maps, through a diffusion-based sampling process. It treats the texture reconstruction problem as an in-painting approach, where off-the-shelf approaches are used to acquire the visible facial texture and geometry. Then, a multi-modal diffusion model is used to complete the non-visible parts of the facial texture maps, as well as reflectance. Relightify retains the visible input during inference, resulting in great performance in identity preservation (Sec. 4.4), which however introduces certain limitations: a) low-resolution images result in low-resolution textures, and b) wearable items (glasses, headbands) partially leak into the reflectance textures, as shown in Fig. 10.

On the contrary, FitDiff concurrently generates facial texture maps and geometry from scratch, and initializes the process from Gaussian noise. This results in a) robust shape and texture reconstruction even under occlusions and accessories, and b) always generating high-quality texture maps. Despite these advantages, our approach performs slightly worse than Relightify in facial texture benchmarks. We sincerely believe that the robustness benefits above make FitDiff an important alternative approach with multiple important use-cases. In fact, our model can actually be used in tandem with Relightify to provide more accurate shape priors to further boost its performance.

On the other hand, the very recent AlbedoGAN [72] is the first model that concurrently generates facial texture and shape. It provides FLAME [50] parameters alongside displacement maps for accurate facial shape reconstruction. While finetuning on the image input, it also produces a facial texture UV map often incorporating baked illumination and accessories. This consequently leads to reduced relightability in the generated avatars. It also replicates the limita-

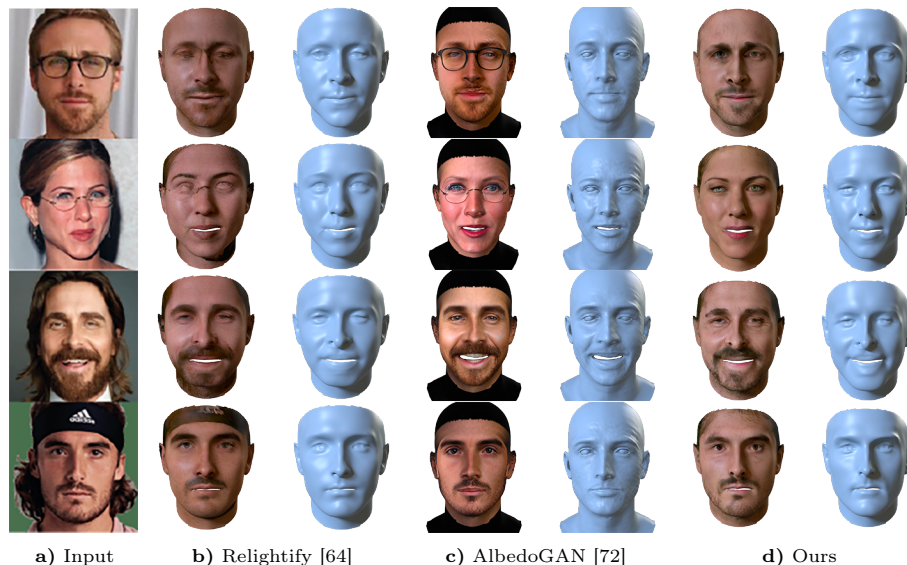


**Fig. 10:** Qualitative comparison with Relightify [64] and AlbedoGAN [72] with FitDiff. Relightify is sensitive to occlusions such as glasses and headbands, while AlbedoGAN only produces one texture and essentially copies the input image, including glasses, teeth and shadows, while our method is robust to both and creates accurate and high-quality reflectance maps, including albedo, normals and specular.

tions observed in Relightify, where wearable items are incorporated into the final facial texture (Fig. 10c). Finally, in comparison with FitMe [44], our experimentation results and qualitative assessments show that our generated texture maps achieve superior performance. We understand that this is due to the necessity in GAN-based fitting methods to meticulously initialize the GAN’s  $\mathbf{z}$  or  $\mathbf{w}$  embedding for back-propagation during inference, in order to mitigate optimization instabilities. The proposed method excels without the need for heuristic priors or regularization terms.

## 7 Conclusion

In this paper, we introduced FitDiff, a diffusion-based 3D facial generative model, conditioned on identity embeddings. Acquiring such embeddings from a powerful pre-trained facial recognition method enables us to capture large variations in ethnicity, age, and gender from a single 2D facial image with no restriction on quality, pose, or illumination. Our method jointly generates facial shapes, facial reflectance maps, and scene illumination parameters. Through a series of experiments, FitDiff showcases state-of-the-art performance in preserving identity and reconstructing facial reflectance, either matching or surpassing established methods. Finally, it exhibits the capability to generate unconditional samples, further highlighting its versatility and effectiveness.

*Acknowledgements:* S. Zafeiriou and part of the research was funded by the EPSRC Fellowship DEFORM (EP/S010203/1) and EPSRC Project GNOMON (EP/X011364/1).

## References

1. Abrevaya, V., Boukhayma, A., Wuhler, S., Boyer, E.: A decoupled 3d facial shape model by adversarial training. In: 2019 IEEE/CVF International Conference on Computer Vision (ICCV). pp. 9418–9427. IEEE Computer Society, Los Alamitos, CA, USA (nov 2019). <https://doi.org/10.1109/ICCV.2019.00951>, <https://doi.ieeecomputersociety.org/10.1109/ICCV.2019.00951>
2. Alexander, O., Rogers, M., Lambeth, W., Chiang, J.Y., Ma, W.C., Wang, C.C., Debevec, P.: The digital emily project: Achieving a photorealistic digital actor. *IEEE Computer Graphics and Applications* **30**(4), 20–31 (2010)
3. Amberg, B., Knothe, R., Vetter, T.: Expression invariant 3D face recognition with a morphable model. In: 2008 8th IEEE International Conference on Automatic Face and Gesture Recognition, FG 2008. pp. 1–6. IEEE (2008). <https://doi.org/10.1109/AFGR.2008.4813376>
4. Athar, S., Xu, Z., Sunkavalli, K., Shechtman, E., Shu, Z.: Rignerf: Fully controllable neural 3d portraits. In: *Computer Vision and Pattern Recognition (CVPR)* (2022)
5. Bagautdinov, T., Wu, C., Saragih, J., Fua, P., Sheikh, Y.: Modeling facial geometry using compositional vaes. In: *Proceedings of the IEEE Conference on Computer Vision and Pattern Recognition*. pp. 3877–3886 (2018)
6. Blanz, V., Vetter, T.: A morphable model for the synthesis of 3d faces. In: *SIGGRAPH '99* (1999)
7. Blattmann, A., Rombach, R., Ling, H., Dockhorn, T., Kim, S.W., Fidler, S., Kreis, K.: Align your latents: High-resolution video synthesis with latent diffusion models. In: *IEEE Conference on Computer Vision and Pattern Recognition (CVPR)* (2023)
8. Booth, J., Roussos, A., Ponniah, A., Dunaway, D., Zafeiriou, S.: Large scale 3d morphable models. *International Journal of Computer Vision* **126**(2), 233–254 (2018)
9. Booth, J., Roussos, A., Zafeiriou, S., Ponniah, A., Dunaway, D.: A 3D morphable model learnt from 10,000 faces. In: *Proceedings of the IEEE Computer Society Conference on Computer Vision and Pattern Recognition*. vol. 2016-December, pp. 5543–5552 (2016). <https://doi.org/10.1109/CVPR.2016.598>
10. Bouaziz, S., Wang, Y., Pauly, M.: Online modeling for realtime facial animation. *ACM Transactions on Graphics* **32**(4), 40 (2013). <https://doi.org/10.1145/2461912.2461976>
11. Breidt, M., Bülthoff, H.H., Curio, C.: Robust semantic analysis by synthesis of 3D facial motion. In: 2011 IEEE International Conference on Automatic Face and Gesture Recognition and Workshops, FG 2011. pp. 713–719. IEEE (2011). <https://doi.org/10.1109/FG.2011.5771336>
12. Bulat, A., Tzimiropoulos, G.: How far are we from solving the 2d & 3d face alignment problem? (and a dataset of 230,000 3d facial landmarks). In: *International Conference on Computer Vision* (2017)
13. Cao, C., Weng, Y., Zhou, S., Tong, Y., Zhou, K.: FaceWarehouse: A 3D facial expression database for visual computing. *IEEE Transactions on Visualization and*

- Computer Graphics **20**(3), 413–425 (2014). <https://doi.org/10.1109/TVCG.2013.249>
14. Chai, Z., Zhang, H., Ren, J., Kang, D., Xu, Z., Zhe, X., Yuan, C., Bao, L.: Realy: Rethinking the evaluation of 3d face reconstruction. In: Proceedings of the European Conference on Computer Vision (ECCV) (2022)
  15. Chai, Z., Zhang, T., He, T., Tan, X., Baltrusaitis, T., Wu, H., Li, R., Zhao, S., Yuan, C., Bian, J.: Hiface: High-fidelity 3d face reconstruction by learning static and dynamic details. In: Proceedings of the IEEE/CVF International Conference on Computer Vision (ICCV). pp. 9087–9098 (October 2023)
  16. Chan, E.R., Lin, C.Z., Chan, M.A., Nagano, K., Pan, B., De Mello, S., Gallo, O., Guibas, L.J., Tremblay, J., Khamis, S., Karras, T., Wetzstein, G.: Efficient geometry-aware 3d generative adversarial networks. In: Proceedings of the IEEE/CVF Conference on Computer Vision and Pattern Recognition (CVPR). pp. 16123–16133 (June 2022)
  17. Dai, H., Pears, N., Smith, W., Duncan, C.: A 3D morphable model of craniofacial shape and texture variation. In: Proceedings of the IEEE International Conference on Computer Vision. vol. 2017-October, pp. 3104–3112 (2017). <https://doi.org/10.1109/ICCV.2017.335>
  18. Deng, J., Guo, J., Xue, N., Zafeiriou, S.: Arcface: Additive angular margin loss for deep face recognition. In: Proceedings of the IEEE/CVF conference on computer vision and pattern recognition. pp. 4690–4699 (2019)
  19. Dhariwal, P., Nichol, A.: Diffusion models beat gans on image synthesis. In: Ranzato, M., Beygelzimer, A., Dauphin, Y., Liang, P., Vaughan, J.W. (eds.) Advances in Neural Information Processing Systems. vol. 34, pp. 8780–8794. Curran Associates, Inc. (2021), [https://proceedings.neurips.cc/paper\\_files/paper/2021/file/49ad23d1ec9fa4bd8d77d02681df5cfa-Paper.pdf](https://proceedings.neurips.cc/paper_files/paper/2021/file/49ad23d1ec9fa4bd8d77d02681df5cfa-Paper.pdf)
  20. Dib, A., Thebault, C., Ahn, J., Gosselin, P.H., Theobalt, C., Chevallier, L.: Towards high fidelity monocular face reconstruction with rich reflectance using self-supervised learning and ray tracing. In: Proceedings of the IEEE/CVF International Conference on Computer Vision. pp. 12819–12829 (2021)
  21. Esser, P., Rombach, R., Ommer, B.: Taming transformers for high-resolution image synthesis. In: Proceedings of the IEEE/CVF Conference on Computer Vision and Pattern Recognition (CVPR). pp. 12873–12883 (June 2021)
  22. Feng, Y., Feng, H., Black, M.J., Bolkart, T.: Learning an animatable detailed 3d face model from in-the-wild images. ACM Trans. Graph. **40**(4) (jul 2021). <https://doi.org/10.1145/3450626.3459936>, <https://doi.org/10.1145/3450626.3459936>
  23. Galanakis, S., Gecer, B., Lattas, A., Zafeiriou, S.: 3dmm-rf: Convolutional radiance fields for 3d face modeling. In: Proceedings of the IEEE/CVF Winter Conference on Applications of Computer Vision (WACV). pp. 3536–3547 (January 2023)
  24. Gao, C., Shih, Y., Lai, W.S., Liang, C.K., Huang, J.B.: Portrait neural radiance fields from a single image. arXiv preprint arXiv:2012.05903 (2020)
  25. Gecer, B., Deng, J., Zafeiriou, S.: Ostec: One-shot texture completion. In: Proceedings of the IEEE/CVF Conference on Computer Vision and Pattern Recognition (CVPR). pp. 7628–7638 (June 2021)
  26. Gecer, B., Lattas, A., Ploumpis, S., Deng, J., Papaioannou, A., Moschoglou, S., Zafeiriou, S.: Synthesizing Coupled 3D Face Modalities by Trunk-Branch Generative Adversarial Networks. In: European Conference on Computer Vision (ECCV) (2020)



27. Gecer, B., Ploumpis, S., Kotsia, I., Zafeiriou, S.: Ganfit: Generative adversarial network fitting for high fidelity 3d face reconstruction. In: Proceedings of the IEEE/CVF Conference on Computer Vision and Pattern Recognition (CVPR) (June 2019)
28. Gecer, B., Ploumpis, S., Kotsia, I., Zafeiriou, S.P.: Fast-ganfit: Generative adversarial network for high fidelity 3d face reconstruction. *IEEE Transactions on Pattern Analysis and Machine Intelligence* (2021)
29. Genova, K., Cole, F., Maschinot, A., Sarna, A., Vlasic, D., Freeman, W.T.: Unsupervised training for 3d morphable model regression. In: Proceedings of the IEEE Conference on Computer Vision and Pattern Recognition (CVPR) (June 2018)
30. Ghosh, A., Fyfe, G., Tunwattanapong, B., Busch, J., Yu, X., Debevec, P.: Multiview face capture using polarized spherical gradient illumination. *ACM Transactions on Graphics (TOG)* **30**(6), 1–10 (2011)
31. Goodfellow, I., Pouget-Abadie, J., Mirza, M., Xu, B., Warde-Farley, D., Ozair, S., Courville, A., Bengio, Y.: Generative adversarial nets. In: Ghahramani, Z., Welling, M., Cortes, C., Lawrence, N., Weinberger, K. (eds.) *Advances in Neural Information Processing Systems*. vol. 27. Curran Associates, Inc. (2014), <https://proceedings.neurips.cc/paper/2014/file/5ca3e9b122f61f8f06494c97b1afccf3-Paper.pdf>
32. Han, Y., Wang, Z., Xu, F.: Learning a 3d morphable face reflectance model from low-cost data. In: CVPR (2023)
33. Ho, J., Jain, A., Abbeel, P.: Denoising diffusion probabilistic models. *arXiv preprint arxiv:2006.11239* (2020)
34. Ho, J., Salimans, T.: Classifier-free diffusion guidance. *arXiv preprint arXiv:2207.12598* (2022)
35. Hong, Y., Peng, B., Xiao, H., Liu, L., Zhang, J.: Headnerf: A real-time nerf-based parametric head model (2022)
36. Huang, G.B., Ramesh, M., Berg, T., Learned-Miller, E.: Labeled faces in the wild: A database for studying face recognition in unconstrained environments. Tech. Rep. 07-49, University of Massachusetts, Amherst (October 2007)
37. Karras, T., Aila, T., Laine, S., Lehtinen, J.: Progressive growing of GANs for improved quality, stability, and variation. In: *International Conference on Learning Representations* (2018), <https://openreview.net/forum?id=Hk99zCeAb>
38. Karras, T., Aittala, M., Hellsten, J., Laine, S., Lehtinen, J., Aila, T.: Training generative adversarial networks with limited data. In: *Proc. NeurIPS* (2020)
39. Karras, T., Laine, S., Aila, T.: A style-based generator architecture for generative adversarial networks. *CoRR* **abs/1812.04948** (2018), <http://arxiv.org/abs/1812.04948>
40. Karras, T., Laine, S., Aittala, M., Hellsten, J., Lehtinen, J., Aila, T.: Analyzing and improving the image quality of StyleGAN. In: *Proc. CVPR* (2020)
41. Kim, G., Kwon, T., Ye, J.C.: Diffusionclip: Text-guided diffusion models for robust image manipulation. In: Proceedings of the IEEE/CVF Conference on Computer Vision and Pattern Recognition (CVPR). pp. 2426–2435 (June 2022)
42. Kodali, N., Abernethy, J., Hays, J., Kira, Z.: On convergence and stability of gans. *arXiv preprint arXiv:1705.07215* (2017)
43. Lattas, A., Moschoglou, S., Gecer, B., Ploumpis, S., Triantafyllou, V., Ghosh, A., Zafeiriou, S.: Avatarme: Realistically renderable 3d facial reconstruction "in-the-wild". In: Proceedings of the IEEE/CVF Conference on Computer Vision and Pattern Recognition (CVPR) (June 2020)

44. Lattas, A., Moschoglou, S., Ploumpis, S., Gecer, B., Deng, J., Zafeiriou, S.: FitMe: Deep photorealistic 3D morphable model avatars. In: Proceedings of the IEEE/CVF Conference on Computer Vision and Pattern Recognition (CVPR) (June 2023)
45. Lattas, A., Moschoglou, S., Ploumpis, S., Gecer, B., Ghosh, A., Zafeiriou, S.P.: Avatarme++: Facial shape and brdf inference with photorealistic rendering-aware gans. *IEEE Transactions on Pattern Analysis & Machine Intelligence* (01), 1–1 (2021)
46. Lei, B., Ren, J., Feng, M., Cui, M., Xie, X.: A hierarchical representation network for accurate and detailed face reconstruction from in-the-wild images (2023)
47. Li, C., Morel-Forster, A., Vetter, T., Egger, B., Kortylewski, A.: Robust model-based face reconstruction through weakly-supervised outlier segmentation. In: Proceedings of the IEEE/CVF Conference on Computer Vision and Pattern Recognition. pp. 372–381 (2023)
48. Li, H., Weise, T., Pauly, M.: Example-based facial rigging. *ACM SIGGRAPH 2010 Papers, SIGGRAPH 2010* **29**(4), 32 (2010). <https://doi.org/10.1145/1778765.1778769>
49. Li, R., Bladin, K., Zhao, Y., Chinara, C., Ingraham, O., Xiang, P., Ren, X., Prasad, P., Kishore, B., Xing, J., Li, H.: Learning formation of physically-based face attributes. In: 2020 IEEE/CVF Conference on Computer Vision and Pattern Recognition (CVPR). pp. 3407–3416. IEEE Computer Society, Los Alamitos, CA, USA (jun 2020). <https://doi.org/10.1109/CVPR42600.2020.00347>, <https://doi.ieeecomputersociety.org/10.1109/CVPR42600.2020.00347>
50. Li, T., Bolkart, T., Black, M.J., Li, H., Romero, J.: Learning a model of facial shape and expression from 4D scans. *ACM Transactions on Graphics, (Proc. SIGGRAPH Asia)* **36**(6), 194:1–194:17 (2017), <https://doi.org/10.1145/3130800.3130813>
51. Lin, C.H., Gao, J., Tang, L., Takikawa, T., Zeng, X., Huang, X., Kreis, K., Fidler, S., Liu, M.Y., Lin, T.Y.: Magic3d: High-resolution text-to-3d content creation. In: Proceedings of the IEEE/CVF Conference on Computer Vision and Pattern Recognition (CVPR). pp. 300–309 (June 2023)
52. Liu, H., Chen, Z., Yuan, Y., Mei, X., Liu, X., Mandic, D., Wang, W., Plumbley, M.D.: Audioldm: Text-to-audio generation with latent diffusion models. *arXiv preprint arXiv:2301.12503* (2023)
53. Liu, Z., Feng, Y., Black, M.J., Nowrouzezahrai, D., Paull, L., Liu, W.: Meshdiffusion: Score-based generative 3d mesh modeling. In: International Conference on Learning Representations (2023), <https://openreview.net/forum?id=0cpM2ApF9p6>
54. Lombardi, S., Saragih, J., Simon, T., Sheikh, Y.: Deep appearance models for face rendering. *ACM Transactions on Graphics* **37**(4), 68 (2018). <https://doi.org/10.1145/3197517.3201401>
55. Luo, H., Nagano, K., Kung, H.W., Xu, Q., Wang, Z., Wei, L., Hu, L., Li, H.: Normalized avatar synthesis using stylegan and perceptual refinement. In: Proceedings of the IEEE/CVF Conference on Computer Vision and Pattern Recognition (CVPR). pp. 11662–11672 (June 2021)
56. Lyu, Z., Kong, Z., Xu, X., Pan, L., Lin, D.: A conditional point diffusion-refinement paradigm for 3d point cloud completion. *ArXiv abs/2112.03530* (2021)
57. Ma, Z., Zhu, X., Qi, G., Lei, Z., Zhang, L.: Otavatar: One-shot talking face avatar with controllable tri-plane rendering. *arXiv preprint arXiv:2303.14662* (2023)

58. Mildenhall, B., Srinivasan, P.P., Tancik, M., Barron, J.T., Ramamoorthi, R., Ng, R.: Nerf: Representing scenes as neural radiance fields for view synthesis. In: European conference on computer vision. pp. 405–421. Springer (2020)
59. Mohamed, S., Lakshminarayanan, B.: Learning in implicit generative models. arXiv preprint arXiv:1610.03483 (2016)
60. Moschoglou, S., Ploumpis, S., Nicolaou, M., Papaioannou, A., Zafeiriou, S.: 3DFaceGAN: Adversarial nets for 3D face representation, generation, and translation. arXiv preprint arXiv:1905.00307 (2019)
61. Nichol, A., Dhariwal, P., Ramesh, A., Shyam, P., Mishkin, P., McGrew, B., Sutskever, I., Chen, M.: Glide: Towards photorealistic image generation and editing with text-guided diffusion models. arXiv preprint arXiv:2112.10741 (2021)
62. Or-El, R., Luo, X., Shan, M., Shechtman, E., Park, J.J., Kemelmacher-Shlizerman, I.: Stylesdf: High-resolution 3d-consistent image and geometry generation. In: Proceedings of the IEEE/CVF Conference on Computer Vision and Pattern Recognition (CVPR). pp. 13503–13513 (June 2022)
63. Papaioannou, A., Gecer, B., Cheng, S., Chrysos, G., Deng, J., Fotiadou, E., Kampouris, C., Kollias, D., Moschoglou, S., Songsri-In, K., et al.: Mimicme: A large scale diverse 4d database for facial expression analysis. In: Computer Vision–ECCV 2022: 17th European Conference, Tel Aviv, Israel, October 23–27, 2022, Proceedings, Part VIII. pp. 467–484. Springer (2022)
64. Paraperas Papantoniou, F., Lattas, A., Moschoglou, S., Zafeiriou, S.: Relightify: Relightable 3d faces from a single image via diffusion models. In: Proceedings of the IEEE/CVF International Conference on Computer Vision (ICCV) (2023)
65. Park, J.J., Florence, P., Straub, J., Newcombe, R., Lovegrove, S.: DeepSDF: Learning continuous signed distance functions for shape representation. In: The IEEE Conference on Computer Vision and Pattern Recognition (CVPR) (June 2019)
66. Park, T., Liu, M.Y., Wang, T.C., Zhu, J.Y.: Semantic image synthesis with spatially-adaptive normalization. In: Proceedings of the IEEE Conference on Computer Vision and Pattern Recognition (2019)
67. Parkhi, O.M., Vedaldi, A., Zisserman, A.: Deep face recognition. In: Xianghua Xie, M.W.J., Tam, G.K.L. (eds.) Proceedings of the British Machine Vision Conference (BMVC). pp. 41.1–41.12. BMVA Press (September 2015). <https://doi.org/10.5244/C.29.41>, <https://dx.doi.org/10.5244/C.29.41>
68. Paysan, P., Knothe, R., Amberg, B., Romdhani, S., Vetter, T.: A 3D Face Model for Pose and Illumination Invariant Face Recognition. In: 2009 Sixth IEEE International Conference on Advanced Video and Signal Based Surveillance. pp. 296–301 (Sep 2009). <https://doi.org/10.1109/AVSS.2009.58>
69. Pinaya, W.H.L., Tudosiu, P.D., Dafflon, J., Da Costa, P.F., Fernandez, V., Nachev, P., Ourselin, S., Cardoso, M.J.: Brain imaging generation with latent diffusion models. In: Mukhopadhyay, A., Oksuz, I., Engelhardt, S., Zhu, D., Yuan, Y. (eds.) Deep Generative Models. pp. 117–126. Springer Nature Switzerland, Cham (2022)
70. Poole, B., Jain, A., Barron, J.T., Mildenhall, B.: Dreamfusion: Text-to-3d using 2d diffusion. arXiv (2022)
71. Radford, A., Kim, J.W., Hallacy, C., Ramesh, A., Goh, G., Agarwal, S., Sastry, G., Askell, A., Mishkin, P., Clark, J., Krueger, G., Sutskever, I.: Learning transferable visual models from natural language supervision. In: ICML (2021)
72. Rai, A., Gupta, H., Pandey, A., Carrasco, F.V., Takagi, S.J., Aubel, A., Kim, D., Prakash, A., De la Torre, F.: Towards realistic generative 3d face models. arXiv preprint arXiv:2304.12483 (2023)

73. Ramesh, A., Pavlov, M., Goh, G., Gray, S., Voss, C., Radford, A., Chen, M., Sutskever, I.: Zero-shot text-to-image generation. CoRR **abs/2102.12092** (2021), <https://arxiv.org/abs/2102.12092>
74. Ranjan, A., Bolkart, T., Sanyal, S., Black, M.J.: Generating 3D faces using convolutional mesh autoencoders. Lecture Notes in Computer Science (including subseries Lecture Notes in Artificial Intelligence and Lecture Notes in Bioinformatics) **11207 LNCS**, 725–741 (2018). [https://doi.org/10.1007/978-3-030-01219-9\\_43](https://doi.org/10.1007/978-3-030-01219-9_43)
75. Ravi, N., Reizenstein, J., Novotny, D., Gordon, T., Lo, W.Y., Johnson, J., Gkioxari, G.: Accelerating 3d deep learning with pytorch3d. arXiv:2007.08501 (2020)
76. Rombach, R., Blattmann, A., Lorenz, D., Esser, P., Ommer, B.: High-resolution image synthesis with latent diffusion models. In: Proceedings of the IEEE/CVF Conference on Computer Vision and Pattern Recognition (CVPR). pp. 10684–10695 (June 2022)
77. Ronneberger, O., Fischer, P., Brox, T.: U-net: Convolutional networks for biomedical image segmentation. CoRR **abs/1505.04597** (2015), <http://arxiv.org/abs/1505.04597>
78. Salimans, T., Goodfellow, I., Zaremba, W., Cheung, V., Radford, A., Chen, X., Chen, X.: Improved techniques for training gans. In: Lee, D., Sugiyama, M., Luxburg, U., Guyon, I., Garnett, R. (eds.) Advances in Neural Information Processing Systems. vol. 29. Curran Associates, Inc. (2016), [https://proceedings.neurips.cc/paper\\_files/paper/2016/file/8a3363abe792db2d8761d6403605aeb7-Paper.pdf](https://proceedings.neurips.cc/paper_files/paper/2016/file/8a3363abe792db2d8761d6403605aeb7-Paper.pdf)
79. Sanyal, S., Bolkart, T., Feng, H., Black, M.: Learning to regress 3D face shape and expression from an image without 3D supervision. In: Proceedings IEEE Conf. on Computer Vision and Pattern Recognition (CVPR). pp. 7763–7772 (Jun 2019)
80. Sinha, A., Song, J., Meng, C., Ermon, S.: D2c: Diffusion-decoding models for few-shot conditional generation. Advances in Neural Information Processing Systems **34**, 12533–12548 (2021)
81. Smith, W.A.P., Seck, A., Dee, H., Tiddeman, B., Tenenbaum, J., Egger, B.: A Morphable Face Albedo Model. arXiv:2004.02711 [cs] (Apr 2020)
82. Sohl-Dickstein, J., Weiss, E.A., Maheswaranathan, N., Ganguli, S.: Deep unsupervised learning using nonequilibrium thermodynamics. 32nd International Conference on Machine Learning, ICML 2015 **3**, 2246–2255 (2015)
83. Song, J., Meng, C., Ermon, S.: Denoising diffusion implicit models. arXiv:2010.02502 (October 2020), <https://arxiv.org/abs/2010.02502>
84. Song, Y., Ermon, S.: Generative modeling by estimating gradients of the data distribution. Advances in neural information processing systems **32** (2019)
85. Song, Y., Ermon, S.: Improved techniques for training score-based generative models. Advances in neural information processing systems **33**, 12438–12448 (2020)
86. Song, Y., Sohl-Dickstein, J., Kingma, D.P., Kumar, A., Ermon, S., Poole, B.: Score-based generative modeling through stochastic differential equations. In: International Conference on Learning Representations (2021), <https://openreview.net/forum?id=PXTIG12RRHS>
87. Taherkhani, F., Rai, A., Gao, Q., Srivastava, S., Chen, X., de la Torre, F., Song, S., Prakash, A., Kim, D.: Controllable 3d generative adversarial face model via disentangling shape and appearance. In: Proceedings of the IEEE/CVF Winter Conference on Applications of Computer Vision (WACV). pp. 826–836 (January 2023)

88. Tewari, A., Bernard, F., Garrido, P., Bharaj, G., Elgharib, M., Seidel, H.P., Perez, P., Zollhofer, M., Theobalt, C.: FML: Face Model Learning From Videos. In: 2019 IEEE/CVF Conference on Computer Vision and Pattern Recognition (CVPR). pp. 10804–10814. IEEE, Long Beach, CA, USA (Jun 2019). <https://doi.org/10.1109/CVPR.2019.01107>
89. Thanh-Tung, H., Tran, T.: Catastrophic forgetting and mode collapse in gans. In: 2020 international joint conference on neural networks (ijcnn). pp. 1–10. IEEE (2020)
90. Thies, J., Zollhöfer, M., Nießner, M., Valgaerts, L., Stamminger, M., Theobalt, C.: Real-time expression transfer for facial reenactment. *ACM Transactions on Graphics* **34**(6), 181–183 (2015). <https://doi.org/10.1145/2816795.2818056>
91. Tran, A.T., Hassner, T., Masi, I., Medioni, G.: Regressing robust and discriminative 3D morphable models with a very deep neural network. In: Proceedings - 30th IEEE Conference on Computer Vision and Pattern Recognition, CVPR 2017. vol. 2017-January, pp. 1493–1502 (2017). <https://doi.org/10.1109/CVPR.2017.163>
92. Tran, L., Liu, X.: On learning 3D face morphable model from in-the-wild images. *IEEE Transactions on Pattern Analysis and Machine Intelligence* pp. 1–1 (2019). <https://doi.org/10.1109/tpami.2019.2927975>
93. Vahdat, A., Kreis, K., Kautz, J.: Score-based generative modeling in latent space. In: Neural Information Processing Systems (NeurIPS) (2021)
94. Vaswani, A., Shazeer, N., Parmar, N., Uszkoreit, J., Jones, L., Gomez, A.N., Kaiser, L.u., Polosukhin, I.: Attention is all you need. In: Guyon, I., Luxburg, U.V., Bengio, S., Wallach, H., Fergus, R., Vishwanathan, S., Garnett, R. (eds.) *Advances in Neural Information Processing Systems*. vol. 30. Curran Associates, Inc. (2017), [https://proceedings.neurips.cc/paper\\_files/paper/2017/file/3f5ee243547dee91fbd053c1c4a845aa-Paper.pdf](https://proceedings.neurips.cc/paper_files/paper/2017/file/3f5ee243547dee91fbd053c1c4a845aa-Paper.pdf)
95. Wang, T., Zhang, B., Zhang, T., Gu, S., Bao, J., Baltrusaitis, T., Shen, J., Chen, D., Wen, F., Chen, Q., et al.: Rodin: A generative model for sculpting 3d digital avatars using diffusion. arXiv preprint arXiv:2212.06135 (2022)
96. Wei, S.E., Saragih, J., Simon, T., Harley, A.W., Lombardi, S., Perdoch, M., Hypes, A., Wang, D., Badino, H., Sheikh, Y.: VR facial animation via multiview image translation. *ACM Transactions on Graphics* **38**(4), 67 (2019). <https://doi.org/10.1145/3306346.3323030>
97. Wood, E., Baltrušaitis, T., Hewitt, C., Johnson, M., Shen, J., Milosavljević, N., Wilde, D., Garbin, S., Sharp, T., Stojiljković, I., et al.: 3d face reconstruction with dense landmarks. In: European Conference on Computer Vision. pp. 160–177. Springer (2022)
98. Wu, J.Z., Ge, Y., Wang, X., Lei, S.W., Gu, Y., Shi, Y., Hsu, W., Shan, Y., Qie, X., Shou, M.Z.: Tune-a-video: One-shot tuning of image diffusion models for text-to-video generation. In: Proceedings of the IEEE/CVF International Conference on Computer Vision (ICCV). pp. 7623–7633 (October 2023)
99. Yang, F., Metaxas, D., Wang, J., Shechtman, E., Bourdev, L.: Expression flow for 3D-Aware face component transfer. *ACM Transactions on Graphics* **30**(4), 1–10 (2011). <https://doi.org/10.1145/2010324.1964955>
100. Yenamandra, T., Tewari, A., Bernard, F., Seidel, H.P., Elgharib, M., Cremers, D., Theobalt, C.: i3dmm: Deep implicit 3d morphable model of human heads. In: Proceedings of the IEEE/CVF Conference on Computer Vision and Pattern Recognition. pp. 12803–12813 (2021)
101. Zeng, X., Vahdat, A., Williams, F., Gojcic, Z., Litany, O., Fidler, S., Kreis, K.: Lion: Latent point diffusion models for 3d shape generation. In: *Advances in Neural Information Processing Systems (NeurIPS)* (2022)

102. Zhang, L., Qiu, Q., Lin, H., Zhang, Q., Shi, C., Yang, W., Shi, Y., Yang, S., Xu, L., Yu, J.: Dreamface: Progressive generation of animatable 3d faces under text guidance. arXiv preprint arXiv:2304.03117 (2023)
103. Zhang, R., Isola, P., Efros, A.A., Shechtman, E., Wang, O.: The unreasonable effectiveness of deep features as a perceptual metric. In: CVPR (2018)
104. Zhang, T., Chu, X., Liu, Y., Lin, L., Yang, Z., Xu, Z., Cao, C., Yu, F., Zhou, C., Yuan, C., Li, Y.: Accurate 3d face reconstruction with facial component tokens. pp. 8999–9008 (10 2023). <https://doi.org/10.1109/ICCV51070.2023.00829>
105. Zhou, L., Du, Y., Wu, J.: 3d shape generation and completion through point-voxel diffusion. In: Proceedings of the IEEE/CVF International Conference on Computer Vision (ICCV). pp. 5826–5835 (October 2021)
106. Zielonka, W., Bolkart, T., Thies, J.: Towards metrical reconstruction of human faces. In: European Conference on Computer Vision. pp. 250–269. Springer (2022)